Delft University of Technology

Analysis and experimental validation of the figure of merit for piezoelectric energy harvesters

Deutz, Daniella B.; Pascoe, John Alan; Schelen, Ben; Van Der Zwaag, Sybrand; De Leeuw, Dago M.; Groen, Pim

Important note
To cite this publication, please use the final published version (if applicable).
Please check the document version above.

Electronic Supplementary Information

Analysis and experimental validation of the figure of merit for piezoelectric energy harvesters

Daniella B. Deutz[1,2]*, John-Alan Pascoe[1,3], Ben Schelen[4], Sybrand van der Zwaag[1], Dago M. de Leeuw[1] and Pim Groen[1,5]

[1] Faculty of Aerospace Engineering, Delft University of Technology, Delft, The Netherlands

[2] University Library, University of Southern Denmark, Odense, Denmark

[3] Department of Aeronautics, Imperial College London, London, United Kingdom

[4] DEMO, Corporate Services, EWI, Delft University of Technology, Delft, The Netherlands

[5] Holst Centre, Eindhoven, The Netherlands

*E-mail: dbd@bib.sdu.dk

Table of Contents

1. Introduction

Section 2 contains the derivation of the maximum transmission coefficient, which is defined as the ratio of output energy over input energy. We show that at low values of the electromechanical coupling coefficient, k^2, the maximum transmission coefficient is the same as the transmission coefficient for maximum output energy, *viz. $k^2/(4-2k^2)$*. At high values of k^2, approaching 1, the maximum transmission coefficient goes to unity instead of $\frac{1}{2}k^2$. We show that this situation is practically irrelevant as a maximum transmission coefficient of unity then corresponds to a negligible output energy.

In Section 3 we calculate the elastic mechanical strain for various geometries of the piezoelectric harvester as a function of applied force. We show that the stored mechanical energy going from a clamped disk to a bimorph cantilever differ by more than 6 orders of magnitude. Consequently, the simple boundary condition of a clamped disk is experimentally the only way to reliably compare the performance of a variety of materials in a piezoelectric energy harvester. Details of the strain energy calculations are presented in Section 4.

A piezometer system, built to quantitatively relate the stored electrical energy with the piezoelectric charge and voltage coefficients, is presented in Section 5. In the geometry of a clamped disc there is no shear or bending, meaning that there is hardly any stored electrical energy. Therefore the piezometer system had to be extremely sensitive; able to detect stored energy in the order of nJ/cm^3. We present the working principle of the piezometer system, the force transfer, the temperature control, and the data extraction.

To validate *dg* as the figure of merit for energy harvesting, we used the intermediate, or unsaturated, polarization states of the piezoceramic PZ27 as a model system. The complete electrical characterization is presented in Section 6. We show the relative dielectric constant, piezoelectric charge coefficient, electromechanical coupling constant, figure of merit, mechanical quality factor and dielectric loss, all as a function of remanent polarization.

In Section 7 we show that the expression for the output energy derived, automatically leads to the expression for the output power of a basic vibration-based generator in resonance, as derived in the seminal paper of Roundy.[1] As a special case, in Section 8, we analyze strain-driven generators

There are many ways to transfer the stored energy electrical energy to the outside world such as diode rings or inductive coils. We did not optimize the electrical-electrical conversion but used a resistive load. A detailed analysis of the equivalent electrical circuit is presented in Section 9. The conversion efficiency is 50%.

2. Maximum transmission coefficient of a piezoelectric harvester

The harvester can be optimized to extract the maximum amount of stored energy, as analyzed in the main text, but it can also be optimized to obtain the maximum transmission coefficient,

λ_{max}. The transmission coefficient, λ, is the ratio of output energy over input energy.[1-3] For a linear transducer:

$$\lambda = \frac{output\ mechanical\ energy}{input\ electrical\ energy} \text{, or equivalently } \lambda = \frac{output\ electrical\ energy}{input\ mechanical\ energy} \tag{S1}$$

We take a piezoelectric capacitor with a mechanical load as with zero mechanical load, or complete clamped conditions (*i.e.* no strain), no energy is sent to the outside world. We take the simplest case where a mass is put on the piezoelectric capacitor. The mechanical load yields a constant compressive stress, X, *i.e.* $X < 0$. The stress of the load induces a strain, x, of sX and an electrical displacement of dX. The electrodes are first grounded to annihilate the excess charges. Then, in order to generate an outside stress, an electric field, E, is applied. This field yields an additional strain of dE. The total strain is then given by:

$$x = sX + dE \tag{S2}$$

and the mechanical output energy is given by:

$$U_{out} = \frac{1}{2}xX = \frac{1}{2}(sX + dE)X \tag{S3}$$

The corresponding input electrical energy follows from the displacement as:

$$U_{elect,in} = \frac{1}{2}DE = \frac{1}{2}\left(\varepsilon_r\varepsilon_0 E + dX\right)E = \frac{1}{2}\left(\varepsilon_r\varepsilon_0 E + d(-\frac{dE}{2s})\right)E \tag{S4}$$

The transmission coefficient is the ratio between output work, *c.f.* eqn. (S3), and input electrical energy, *c.f.* eqn. (S4), and reads:

$$\lambda = -\frac{1}{2}(dE + sX)X \Big/ \frac{1}{2}\left(\varepsilon_r\varepsilon_0 E + dX\right)E = -(dg + sg^2)/(\varepsilon_r\varepsilon_0 + dg) \tag{S5}$$

where g is taken as X/E. Following Ref.[2,3], the value of g where the transmission coefficient is maximum, is obtained from $d\lambda/dg$ is zero and derived as:

$$g_{max} = (X/E)_{max} = (\varepsilon_r\varepsilon_0/d)\left(-1 \pm \sqrt{(1 - k^2)}\right) \tag{S6}$$

We take only the positive sign, as the negative sign leads to a second derivate smaller than zero. The limiting values for $k \to 0$ and $k \to 1$ are:

$$\lim_{k=0} g_{max} = -1/2(\varepsilon_r\varepsilon_0/d)k^2 = -d/2s \tag{S7}$$

$$\lim_{k=1} g_{max} = -(\varepsilon_r\varepsilon_0/d) = -d/s \tag{S8}$$

Meaning that the maximum transmission coefficient is obtained at low values of k^2 when the strain induced by the external load is half of the strain generated by the electric field, and for

3

values of k^2 approaching unity the strain induced by the external load is equal to the strain generated by the electric field. Putting the value for g_{max} in the transmission coefficient leads to:

$$\lambda_{max} = - \left(dg - \frac{1}{d} * (2\varepsilon_r\varepsilon_0 sg + \varepsilon_r\varepsilon_0 d)\right)/(\varepsilon_r\varepsilon_0 + dg) \tag{S9}$$

which can be rewritten as

$$\lambda_{max} = - \left(dg\left(\frac{2}{k^2} - 1\right) + \varepsilon_r\varepsilon_0 \right)/(\varepsilon_r\varepsilon_0\sqrt{(1 - k^2)}) \tag{S10}$$

$$= \frac{2}{k^2} - 1 - \frac{2}{k^2} * \sqrt{(1 - k^2)} \tag{S11}$$

$$= \left(1/k - \sqrt{(1/k)^2 - 1}\right)^2 = \left(1/k + \sqrt{(1/k)^2 - 1}\right)^{-2} \tag{S12}$$

where we have used:

$$\left(\frac{1}{k} - \sqrt{\frac{1^2}{k} - 1}\right) * \left(\frac{1}{k} + \sqrt{\frac{1^2}{k} - 1}\right) = 1 \tag{S13}$$

At small values of k^2, λ_{max} can be approximated as:

$$\lambda_{max} = \left(1/k + \sqrt{(1/k)^2 - 1}\right)^{-2} \cong k^2/(4 - 2k^2) \tag{S14}$$

which is equal to the transmission coefficient derived for the maximum output energy, *c.f.* eqn. (14) as derived in the main manuscript.

The electrical input energy for the maximum transmission coefficient is calculated using eqn. (S6) for g_{max} as:

$$U_{elec} = k^2 \sqrt{(1 - k^2)} \left(-1 + \sqrt{(1 - k^2)}\right)^{-2} * \frac{1}{2}sX^2 = \sqrt{(1 - k^2)}/\lambda_{max} * \frac{1}{2}sX^2 \tag{S15}$$

which leads to the corresponding output energy:

$$U_{output} = \lambda_{max}U_{elec} = \sqrt{(1 - k^2)} * \frac{1}{2}sX^2 \tag{S16}$$

For low values of k^2, below about 0.6, the maximum transmission coefficient is the same as the transmission coefficient for maximum output energy, *viz.* $k^2/(4-2k^2)$. Furthermore, the expressions for both input and output energy are similar. Maximum output energy and maximum transmission coefficient are obtained when the strain of the mechanical load is half the electrically generated strain, *i.e.* X/*E* is equal to *-2d/s*.

At very high values of k^2, approaching 1, there is a difference. The maximum transmission coefficient goes to unity instead of $\frac{1}{2} k^2$. However, the maximum transmission coefficient is realized when the strain of the load is about equal to the strain due to the electric field. The total strain, and, hence, the output power both go to zero, as described by eqn. (S12). Therefore, this situation is practically irrelevant. A classical problem, the maximum transmission coefficient is unity but under that constraint you cannot harvest energy. At high k^2 don't go for the maximum transmission coefficient but simply harvest the maximum output energy.

3. Stored electrical energy and input mechanical energy

In this work, the maximum stored electrical energy, for a single sinusoidal excitation, has consistently been in the order of nJ/cm^3. However, output powers of vibrational energy harvesters are commonly reported in the order of mW/cm^3. The discrepancy is due to the boundary conditions of the mechanical load, as will be discussed below.

We measured the stored electrical energy of different material classes in the simple boundary condition of a clamped disk. This is experimentally the only way to reliably compare a variety of piezoelectric materials under identical conditions. However, we note that this clamped condition is the least efficient at transferring the applied load into elastic strain energy. The calculated elastic strain energy of a clamped plate, of dimensions 1 x 1 x 0.1 cm, is shown in Fig. S1a as a function of applied force. At 10 N, only 5.95 nJ of elastic strain energy is induced. We derive an electromechanical coupling coefficient, k^2, of 0.36, by dividing the measured stored electrical energy over the calculated mechanical strain energy of the PZ27 disk. This value is in perfect agreement with the measured value of 0.35, as shown in ESI Section 6, and with reported values for PZT piezoceramics. Hence, we can conclude that the calculated strain energy in a clamped disk is a good approximation for the actual strain energy.

To increase the stored electrical energy of the piezoelectric material, the mechanical boundary conditions must be changed in order to induce more elastic strain energy per applied force. To this end we calculated the stored mechanical energy for a fixed volume of piezoelectric material, by varying only the shape and clamping conditions. For six different configurations, shown in Fig. S1b, the strain energy as a function of applied force is presented in Fig. S1a. Details of the calculations are presented in ESI Section 4.

In the first example, we changed the clamped plate into a simply supported plate of the same dimensions. As the plate can bend in the center, the strain energy immediately increases by three orders of magnitude, as shown by the dash-dotted light blue curve in Fig. S1a.
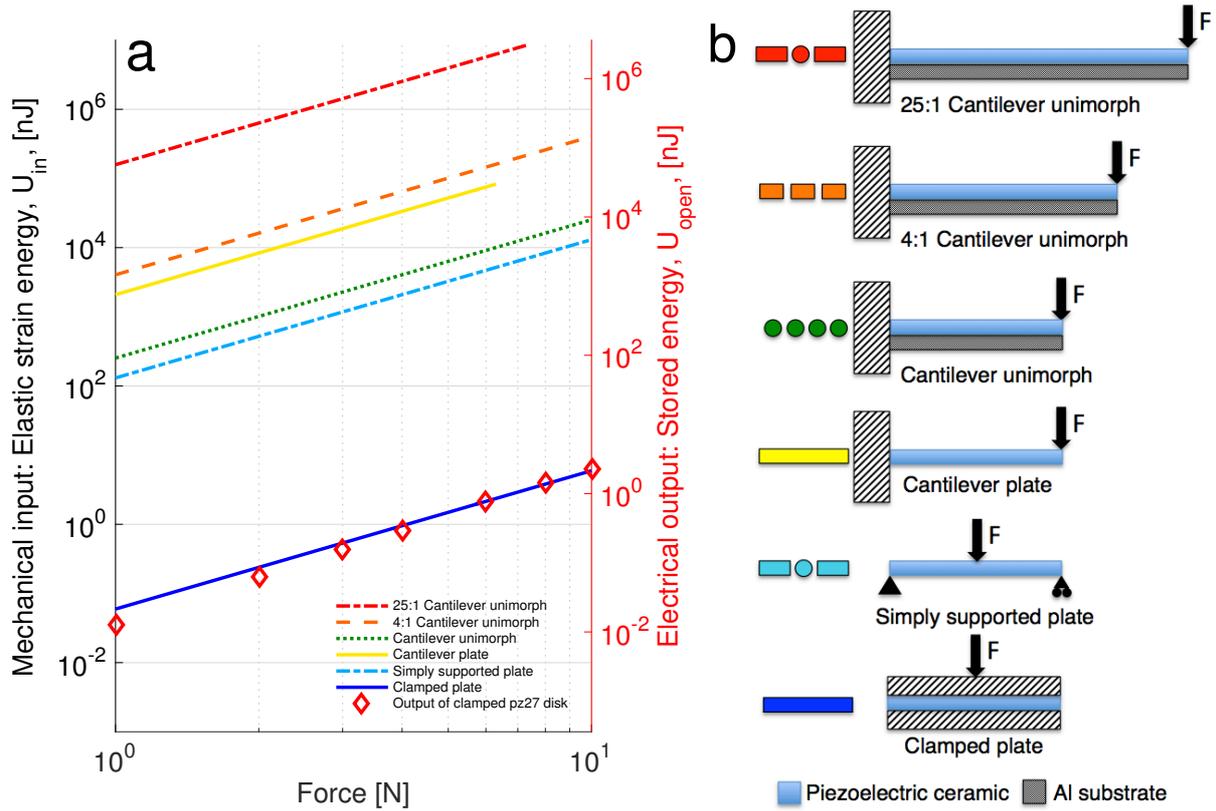
Figure S1. *Calculated mechanical input energy and electrical output energy of 0.1 cm³ volume of piezoelectric material, in six boundary conditions. (a) Elastic strain energy of common piezoelectric energy harvesting components. The open diamond markers represent the measured stored electrical energy of a clamped PZ27 disk, reproduced from the main text in Fig. 4. (b) Graphical representations of the boundary conditions of the analytically calculated piezoelectric plates. From bottom to top: a clamped plate, a simply supported plate, a cantilever plate, a cantilever unimorph, a 4:1 cantilever unimorph where the length of the plate is 4 times its width, and a 25:1 cantilever unimorph with length 25 times its width. The depictions of the cantilever unimorphs with altered geometric ratios are not to scale. The unimorph substrate is scaled such that the neutral axis of the stress is at the bottom of the piezoelectric layer.*

To get even more bending, we exchanged the simply supported plate by a cantilever plate. The strain energy is now even 4.5 orders of magnitude larger, as shown by the yellow, mid-range solid curve in Fig. S1a. The curve abruptly ends at 6.3 N of force, since applying higher forces exceeds the critical tensile stress, X_{crit}, of 34.2 MPa at which the expected probability of failure of this ceramic is 1%.[4] Soft PZT ceramics can withstand higher compressive strain than tensile strain, so to ensure the full volume of the piezoelectric ceramic material is in compression, a unimorph configuration is used.

To calculate the strain energy of the unimorph, we take the same volume of piezoelectric material and assume it is perfectly bonded to an Al plate of equal width and length. To ensure that the piezoelectric plate is in compression, the thickness of the Al plate is chosen such that the neutral axis of the unimorph coincides with the interface between the piezoelectric plate

and Al substrate. The unimorph configuration induces about an order of magnitude less strain energy than the cantilever plate, as can be seen from the dotted curve in Fig. S1a. However, although the stored energy is slightly less, the unimorph can withstand higher absolute strain.

Still more elastic strain energy can be induced in the same volume of piezoelectric material by changing the geometric ratio of the cantilever unimorph, *i.e.*, making it longer and less wide (shown by the top two curves in Fig. S1a. We note that the critical *compressive* strain, is reached at 7.4 N in the cantilever unimorph with a 25:1 geometric ratio. This type of component configuration more closely resembles the piezoelectric harvesters used in literature. For example, at 1 N of applied force, the cantilever unimorph with a geometric ratio of 25:1 achieves 1.6 mJ/cm^3 of strain energy. Assuming the electromechanical coupling is unaffected by the change in boundary conditions from a clamped plate to a cantilever unimorph, the stored electrical energy is expected to be about 0.58 mJ/cm^3. When the piezoelectric component is actuated at 10 Hz, under the same measurement conditions used in this work, the stored electrical power would then be 5.8 mW/cm^3. We note that this order of magnitude perfectly fits the reported estimations for the generated power per unit volume.[5, 6]

4.   Calculation of elastic strain energy as a function of geometric boundary conditions

For a square plate of dimensions of length, L, equal to the breadth, b, of 10 mm and thickness, t, of 1 mm, the formula for the elastic strain energy, U, is given for each geometric boundary condition described in the S.I Section 3. For a clamped plate, U is calculated from the closed form solution as:

$$U = \frac{F^2 t}{2AY}$$
(S17)

where F is the applied force, A is the area and Y is the Young's modulus. There are no closed form solutions for the other cases investigated here, such as simply supported and cantilever boundary conditions. Thus approximations were used, based on the approaches presented in Young and Budynas.[7]

We approximated simply supported and cantilever plates as wide beams. In this case the stiffness needs to be corrected by replacing the Young's modulus with $Y/(1-v^2)$, where v is the Poisson ratio. This approximation is, strictly speaking, only valid if the plate is loaded by a line load. For the simply supported beam loaded in a point by a concentrated load the use of an effective width has been suggested.[7] This adjustment is applied; and increases the calculated strain energy by a factor of 1/0.568, as compared to the value found using regular beam theory. For a cantilever plate under point loading, Young and Budynas[7] present a method that has been validated only for cases where the width of the plate (*i.e.* measured along the clamped side) is greater than 4 times the length (the dimension perpendicular to the clamped edge). The use of this method leads to a decrease in calculated strain energy of about a factor 2 at the maximum applied force, as compared to treating the plate as a beam with the adjusted Young's modulus. We note that these approximations may result in an error of at

most a factor of 2. This factor can be disregarded as the strain energy varies orders of magnitude upon the boundary conditions

For a simply supported plate, the strain energy, U, can be calculated from the well-known equation of deflection of a simply supported beam[8] by using the corrected Young's modulus as follows:

$$U = \frac{(1-v^2)}{Y}\frac{F^2L^3}{96I}; \quad I = \frac{bt^3}{12} \tag{S18}$$

where I is the area moment of inertia.

For the cantilever plate, the strain energy, U, can be calculated analogously, in the same way, from standard beam theory[8] with the corrected Young's modulus:

$$U = \frac{(1-v^2)}{Y}\frac{F^2L^3}{6I} \tag{S19}$$

The unimorph configuration examined here is composed of a PZ27 plate perfectly bonded to an Al plate of equal width. The neutral axis of the unimorph coincides with the interface between the piezoelectric and Al plates. In this way the full volume of the piezoelectric plate experiences compressive stress. The Al plate thickness is then given by:[8]

$$t_{Al} = t_{PZ27}\sqrt{Y_{PZ27}/Y_{Al}} \tag{S20}$$

To calculate the strain energy of this unimorph configuration, we analytically transform the bi-material beam into an equivalent beam made entirely of Al. To compensate for the difference in Young's modulus between the PZ27 ceramic and Al, the width of the part of the beam formerly made of piezoceramic is increased, by a factor Y_{PZ27}/Y_{Al}.

A difference in the Poisson's ratio of the two materials in a unimorph geometry will cause non-uniform strain in thickness direction, resulting in in-plane stresses.[7] The plate will be somewhat stiffer than when the Poisson's ratios are the same, lowering the strain energy for a given force. We note that the difference in the Poisson's ratio of Al (0.33) and PZ27 ceramics (0.35) is small, therefore the effect on the strain energy, for a given force, can be disregarded.

The equations for the strain energy of simply supported and cantilever plates remain valid for the unimorph configuration, with the following modifications: for Y and v the properties of Al are used and I is replaced with:

$$I = \left(\frac{Y_{PZ27}}{Y_{Al}}\right)\frac{bt_{PZ27}^3}{3} + \frac{bt_{Al}^3}{3} \tag{S21}$$

5. Piezometer system to measure the stored electrical energy

A piezometer system was built to quantitatively relate the stored electrical energy with the piezoelectric charge and voltage coefficients, d and g. As discussed in ESI Section 3, and shown in Fig. S1, the elastic, mechanical energy varies over 6 orders of magnitude depending on the geometric boundary conditions. The only way to reliably extract the piezoelectric constants is by using a circular clamped disc. However, in this geometry there is no shear or bending, meaning that there is hardly any stored electrical energy. Therefore the piezometer system had to be extremely sensitive; able to detect stored energy in the order of nJ/cm^3. Here we present the working principle of the piezometer system, the force transfer, the temperature control, and the data extraction. We note that the small stored electrical energies can be accurately determined because the applied force is accurately applied. Consequently, the system developed allows accurate measurement of the stored electrical energy for any piezoelectric material.

The schematic representation of the piezometer system, operating under quasi-static load, is for completeness reproduced from the main manuscript as Fig. S2a. A photograph of the jig is presented in Fig. S2b. An electrical diagram of the system is presented in Fig. S2c.
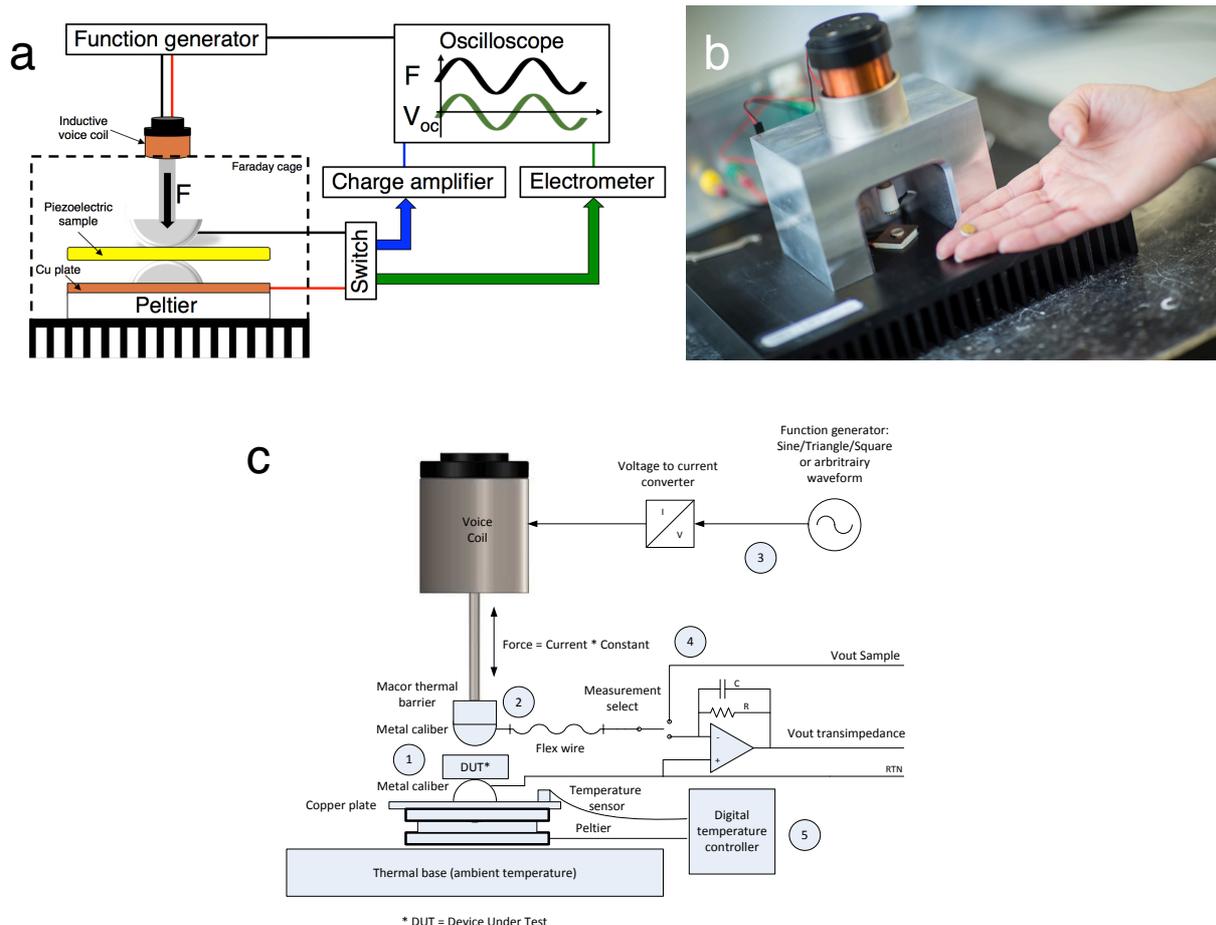

Figure S2. Developed *piezometer system. (a) Schematic representation of the measurement system. (b) Picture of the jig. (c) Schematic diagram of the system, showing a simplified diagram of the peripheral electronics.*

5.1. Working principle of the piezometer system

The piezoelectric sample is placed between two rounded PM300 Piezometer (Piezotest, London, UK) calibers (bubble 1, in Fig. S2c). The sample is metallized on both sides, yielding a piezoelectric capacitor. An inductive voice coil (bubble 3, Fig. S2c), driven by a dynamic electrical signal from an Agilent 33210A function generator (Santa Clara, CA, USA), supplies the source of both static and dynamic force, $F(\omega t) = F_{max} f(\omega t)$, where $f(\omega t)$ is a periodic function (for example, $sin(\omega t)$), t is the time and ω the angular frequency. The polarization of the sample is in line with the direction of the force. The dynamic force generates piezoelectric charges on the surfaces of the piezoelectric sample, $Q(\omega t) = Q_{max} f(\omega t)$.[9]

To measure the short circuit current, $I_{SC}(\omega t)$, the charges $Q(\omega t)$ are lead to an ultra-low noise amplifier that virtually shorts the sample (zero volts over the sample) and converts the current from the sample into a voltage (trans impedance). The gain can be controlled over 4 decades: 1 MΩ, 10 MΩ, 100 MΩ, and 1 GΩ. The electrical bandwidth is limited with a 3rd order Bessel roll off (60 dB per decade) at 5 kHz. A Bessel function is used to get a constant phase delay over frequency, resulting in an overshoot free step electrical function response.

To measure the open circuit voltage, $V_{OC}(\omega t)$, the amplifier is bypassed with a measurement select switch (bubble 4, Fig. S2c). The charges, $Q(\omega t)$, are lead along a guarded cable to a Keithley 6517b Electrometer (Cleveland, OH, USA). The guard function of the electrometer is used to compensate for the capacitance of the coaxial connection between the piezoelectric capacitor and the electrometer.

5.2. Force transfer

The force of the voice coil is applied to the sample through a metal rod, isolated by a Macor mount, and connected to one of the Berlincourt calibers (bubble 2, Fig. S2c). The Macor mount provides electrical and thermal isolation from the samples to the rod, while maintaining rigid transfer of the force to the sample. The offset voltage of the function generator supplies the static force to the sample. A voltage to current converter (amplifier) drives the voice coil up to + or - 20 N with 5 kHz electrical bandwidth. The overall transfer equals 2 N/V.

The applied force to the piezoelectric sample is accurately defined by the current through the voice coil, multiplied with the coil's force constant (in N/A). Under static conditions 100% of the force from the voice coil is transferred to the surface of the sample. The force constant of the voice coil is non-linear when the coil is driven at large strokes. Therefore, to ensure the force is always defined within 5%, the maximum sample thickness is limited to 7 mm (nominal 2 mm + 5 mm).

Under dynamic conditions any elasticity or backlash, between the voice coil and the contact of the mechanical tip of the rod to the sample, will lead to mechanical energy loss. Severe losses occur when the movement of the coil exceeds 10 μm movement at a frequency of 110

Hz. Due to elasticity and backlash, this excitation introduces a force loss of -0.74 N, as calculated from $F_{Loss} = -\omega^2 Am$, where A is the amplitude of the movement, and m is the moving mass of the voice coil, taken as 0.155 kg. The indentation of the mechanical tip of the rod, δ_{tip}, depends on the elasticity of the piezoelectric material being tested, according to: $\delta_{tip} = Ft/A_{caliber}Y$, where $A_{caliber}$ is the contact area of the caliber. Force loss is negligible when measuring rigid piezoceramics since the indentation at the maximum dynamic force of 10 N, is only 0.04 µm. In rubbery materials a 10 µm indentation already occurs at a dynamic force of 0.3 N. Therefore, the measurement frequency is limited to 10 Hz. The maximum force loss for the materials measured here, was -0.10 N for rubbery piezoelectric disks measured at 10 N dynamic force at 10 Hz. Furthermore, to dampen backlash the mount of the voice coil is designed to be extremely rigid.

5.3. *Temperature control*

To study the effect of temperature with force excitation, the device is equipped with a Peltier heating and cooling element, accurately controlled within 1 °C over a temperature range of -10 °C to +100 °C. The temperature is regulated by a MCPE1-07106NC-S Peltier actuated temperature controller, placed beneath a copper plate, sealed to the bottom caliber (bubble 5, Fig. S2c). The copper plate mounts a solid state temperature sensor that is used to create a uniform temperature distribution. The bottom electrode stack can handle extreme forces without compression. To keep the temperature stable, the measured temperature is compared with the desired setpoint and the difference is amplified by a PID-controller that drives the Peltier element. The Peltier element is able to heat and cool with a $\Delta T/\Delta t$ of 20 K/s over a range of -10 °C to 100 °C.

5.4. *Data extraction*

The periodic input waveform, generated by a function generator, and the piezoelectric output waveform, are collected with a DSOX2002A oscilloscope (Tektronix Inc., Berkshire, UK). The open circuit output voltage and short circuit output current were measured under sinusoidal excitation. The peak-to-peak value of the applied force and output were obtained in the frequency domain by using a fast Fourier transform. Only the set frequency was used, and all other signals were disregarded.

6. Electrical characterization of a piezoceramic PZ27 disk as a function of remanent polarization, P_r.

To validate dg as the figure of merit for energy harvesting, we used the intermediate, or unsaturated, polarization states of the piezoceramic PZ27 as a model system. The complete electrical characterization is presented in Fig. S3, where we show the relative dielectric constant, piezoelectric charge coefficient, electromechanical coupling constant, figure of merit, mechanical quality factor and dielectric loss, all as a function of remanent polarization.

The electromechanical coupling coefficient, k_p, and mechanical quality factor, Q_m, were determined by the IEEE resonance method using an Agilent HP4194A impedance analyzer (Santa Clara (CA), USA). The Q_m, is evaluated from the resonance peak in the frequency dependence of the real part of the impedance, Z', via $Q_m = f_{peak} /(f_1 - f_2)$, where f_1 and f_2 are the frequencies at which the impedance is equal to $Z'_{peak}/\sqrt{2}$, and f_{peak} is the frequency at the peak, Z'_{peak}. The k_p was evaluated from the following equation, where f_s and f_p are the series and parallel resonance frequencies.[54]

$$k_p = \frac{\pi}{2} \frac{f_s}{f_p} tan \left(\frac{\pi}{2} \frac{\Delta f}{f_p} \right) \tag{S22}$$

The values of d_{33} are presented as a function of the remanent polarization in the main text as Fig. 2b and here in Fig. S3b. A linear dependence is obtained, with a slope of 1.0 10^{-9} m^2/ N. The order of magnitude can be explained as follows. The origin of intrinsic piezoelectricity is electrostriction, biased by the spontaneous polarization. The piezoelectric strain of a ferroelectric, single domain, single crystal, with a centrosymmetric paraelectric phase, can be obtained from expansion of the free energy in a Taylor series[10] with respect to the electric displacement which is taken as the fundamental variable.[11] As odd terms in the expansion vanish by symmetry,[12] the strain as a function of electric field is given by:[13]

$$X_{33} = Q_{33}D^2 = Q_{33}(\varepsilon_r \varepsilon_0 E\acute{p} + P_s)^2 = 2Q_{33}\varepsilon_r \varepsilon_0 P_s E\acute{p} + Q_{33}P_s^2 + Q_{33}\varepsilon_r^2 \varepsilon_0^2 E^2 \tag{S23}$$

where $\acute{p}$ is a parity function, with values of -1 or +1, to account for the relative orientation of electric field and spontaneous polarization, and where we have used that $\acute{p}^2$ equals unity. Q_{33} is the coefficient of electrostriction, a universal property of solid and liquid dielectrics.[14, 15] The first term on the right hand side of eqn. (S23) corresponds to the piezoelectric effect, with the piezoelectric charge coefficient, d_{33}, given by $2Q_{33}\varepsilon_r \varepsilon_0 P_s$. The piezoelectric effect can thus be understood as the electrostriction biased by the spontaneous polarization. The second term, $Q_{33}P_s^2$, describes the residual, spontaneous strain. The last term, $Q_{33}\varepsilon_r^2 \varepsilon_0^2 E^2$, is referred to as the pure electrostrictive contribution. For ferroelectric materials this term is small and typically disregarded.

Of course the piezoceramic PZ27 is not a single crystal, but the analysis gives a first order explanation for the dependence of d_{33} on the remanent polarization. As shown in Fig. S3, the relative dielectric constant slowly increases with increasing remanent polarization. We take an average value of 1500. For Q_{33} we use the reported value of 0.02 m^4/N^2.[16] The slope of Fig. 2b, $2Q_{33}\varepsilon_0\varepsilon_r$, then is calculated as 5 10^{-10} m^2/N, about half the extracted experimental value. Therefore, about half of the piezoelectric charge coefficient is intrinsic, due to electrostriction biased by the spontaneous polarization, and the other half is extrinsic due to *e.g.* domain wall motion.
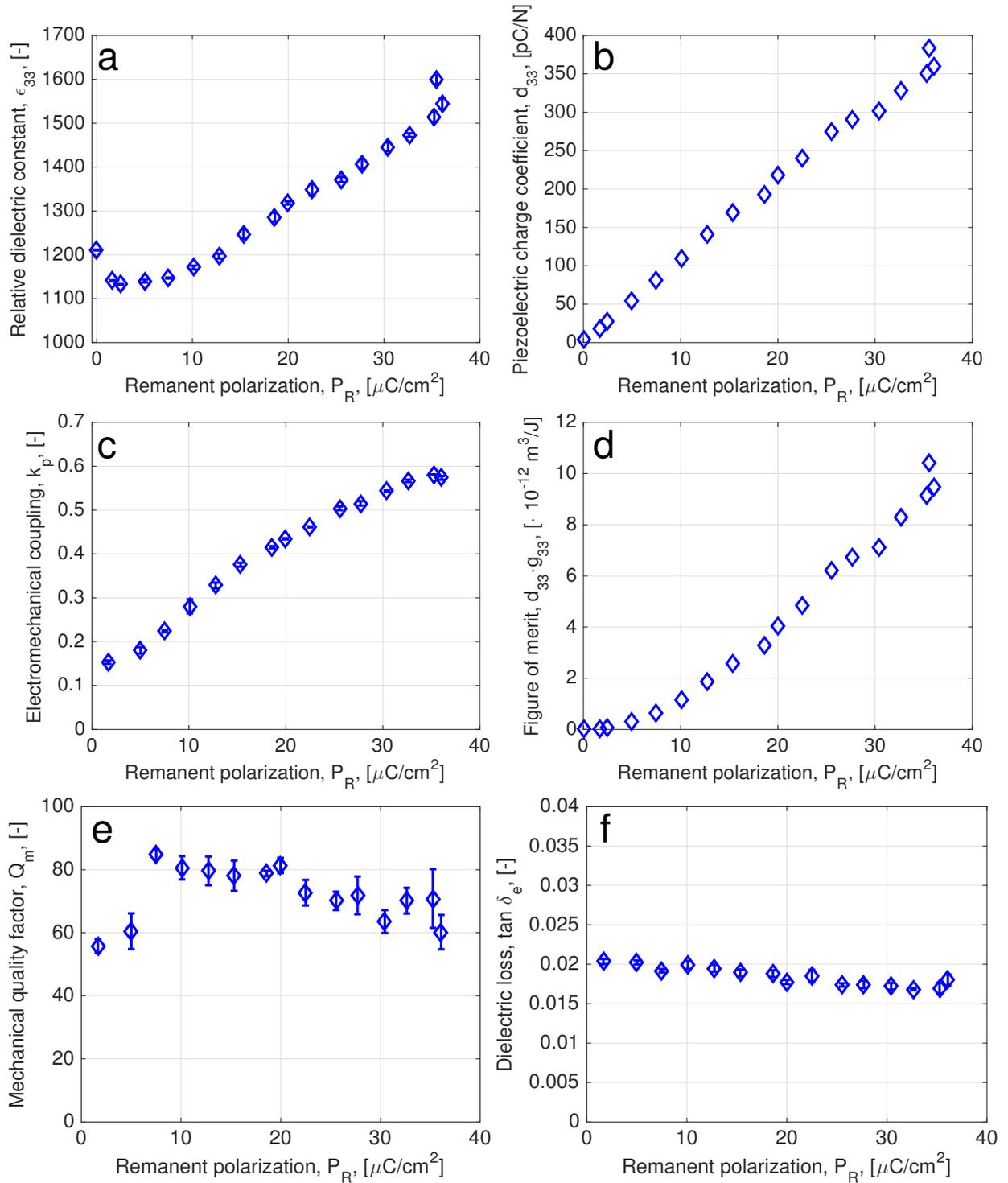
Figure S3. *Electrical performance of a thermally de-poled PZ27 ceramic disk as a function of poling state, signified by the ferroelectric remanent polarization, P_R. (a) Relative dielectric constant, ε_r. (b) Piezoelectric charge coefficient, d_{33}. (c) Electromechanical coupling, k_p. (d) Figure of merit, $d_{33}g_{33}$. (e) Mechanical quality factor, Q_m. and (f) Dielectric loss, $\tan \delta_e$.*

7. Technology independent archetypical generator

Here we show that the expression for the output energy derived, automatically leads to the expression for the output power of a basic vibration-based generator in resonance, as derived in the seminal paper of Roundy.[1]

We approximate an energy harvester as schematically shown in Fig. S4 by a mass, m, coupled to an oscillating spring.[1]
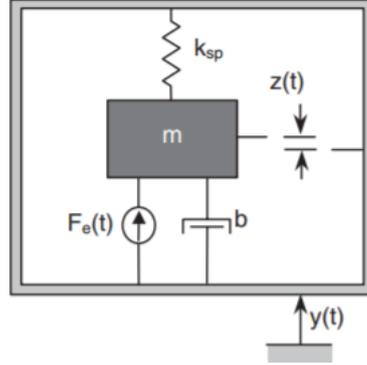

Figure S4. *Schematic of a basic piezoelectric vibration based harvester. $F_e(t)$ is the force generated by the mechanical-electrical coupling, k_{sp} is the spring constant, b is the damping coefficient, y(t) is the displacement of the input vibrations and z(t) is the spring deflection. Reproduced from Roundy.[1]*

We approximate the generated power, P_{max}, from the output energy per cycle, times the resonance frequency ω. As derived in the submitted manuscript, the output energy per cycle is taken as: *$1/(4-2k^2)*1/2dgX^2$*. We take the prefactor, *$1/(4-2k^2)$*, equal to ½ and take 100% for the electrical-electrical conversion. The applied stress, *X*, is equal to *mQA/a* where Q is the quality factor, A is the acceleration and a is the area of the cross section of the mass. We take for the resonance frequency, *ω:*[1]

$$\omega^2 = Ya/mh \tag{S24}$$

where h is the height of the mass and Y is the Young's modulus. The maximum output power is then derived as:

$$P_{max} = \frac{1}{4}dgX^2 * \omega = \frac{1}{4}dg\frac{\omega^2}{\omega}\left(\frac{mQA}{a}\right)^2 = \frac{1}{4}\frac{k^2}{\omega}\frac{m}{ah}(QA)^2 = \frac{k^2\rho(QA)^2}{4\omega} \tag{S25}$$

where ρ is the specific mass, *m/ah*. We note that eqn. (S25) is similar to the expression of maximum output power as derived in the seminal work of Roundy.[1] Furthermore, the same expression is used by many other others, such as.[17-19] We note that a similar expression, for the optimum power of piezoelectric vibrational harvesters with sinusoidal vibrations, has been reported by Renaud.[20] In this paper a crucial and clear distinction is made between the *effective* electromechanical coupling coefficient, K^2, of the complete device, and the electromechanical coupling coefficient of the piezoelectric material alone, k^2.

14

It is remarkable that the formula we derived for the electrical output energy, per sinusoidal excitation, automatically leads to a perfect description of the output power of a basic resonant piezoelectric harvester. This correspondence strongly supports the analysis presented in the main manuscript.

We note that in literature, K^2Q is presented as the FOM of a real harvesting device, with K^2 as the device electromechanical coupling.[20-22] However, K^2Q is typically the FOM of the transformation efficiency of the complete transducer. This FOM is often used to optimize the available output power for a given material combination in a harvester. This is not necessarily the same as the FOM of the absolute optimal output power, or generation efficiency, which is needed to select optimum piezoelectric materials.

8. Strain-driven generator

Our target is to arrive at a piezoelectric generator that delivers sustainable energy to power wireless sensor networks. The output energy of a generator is only a fraction of the environmental input energy. Therefore, we maximized the output energy under the boundary condition of a limited input energy.

On the other hand, energy can be harvested under the boundary condition of basically infinite input energy. Not surprisingly, the figure of merit of those generators is completely different. A typical example is a generator fixed onto a solid support, which creates not a fixed stress, but a fixed strain in the piezoelectric material; for instance a piezoelectric capacitor glued onto a wing of an airplane. Bending of the wing leads to a fixed strain, x, independent of the type of piezoelectric material. The generated electrical energy in open circuit conditions is then:

$$U_{elec,open} = \frac{1}{2}dgX^2 = \frac{1}{2}dgY^2x^2 = k^2 * \frac{1}{2}Yx^2 = k^2 U_{mech\,input} \qquad \text{(S26)}$$

where Y is the Young's modulus. The figure of merit, for this specific strain-driven application which takes the strain as the variable quantity, is then dgY^2, or k^2Y. The reason can easily be understood. The strain is fixed. The mechanical stored energy scales with the Young's modulus. As k^2 is a material parameter, the electrical energy scales with the strain x as k^2Y. For this strain-driven application, piezoelectric materials with a large Young's modulus such as ceramics are indicated. Flexible composite materials are no option. The larger the Young's modulus, the larger is the stored mechanical energy for the given stress; and, concomitantly, the larger is the stored electrical energy. However, the overall efficiency of the harvester is close to zero, as all the vibrational input energy is stored as mechanical energy in the support. Therefore, a strain-driven harvester is no option to efficiently harvest energy from ambient vibrations.

9. Electrical-electrical conversion efficiency of piezoelectric energy harvesting with a resistive load

A resistive load, R_{load}, is placed in parallel to the piezoelectric capacitor to harvest the stored electrical energy. The corresponding equivalent electric circuit is presented in Fig. S5. The piezoelectric capacitor is treated as a current source, I_{in}, actuated with an applied force over time, $F(\omega t) = F_{max} f(\omega t)$, where $f(\omega t)$ is a periodic function (for example, $sin(\omega t)$), where t is the time and ω the angular frequency. The developed current, I_{in}, is the sum of the current due to the internal capacitance, I_{cap}, and the external load, I_{load}.
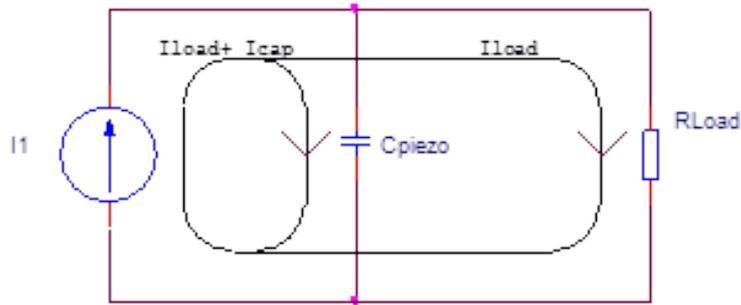

Figure S5. *Equivalent circuit of a piezoelectric capacitor in parallel with a resistive load.*

The harvested output power, P, of the circuit is related to the square of the output voltage, $V_{harvested}$, and the value of the resistive load through:

$$P = \frac{V_{harvested}^2}{R_{load}} = \frac{\left(\left|\frac{I_{in}R_{load}}{1+j\omega C_{piezo}}\right|\right)^2}{R_{load}} \tag{S27}$$

where C_{piezo} is the internal capacitance of the piezoelectric material, and j is $\sqrt{-1}$.

As an example, the power output of a PZ27 ceramic, actuated with a sinusoidal excitation at 10 Hz and 3 N peak to peak, is presented in Fig. S6a. The piezoelectric disk has a capacitance of 1145 pF. The calculated power output *c.f.* eqn. (S27) takes the form of a parabola, at values of the resistive load between 10^6 and 10^8 Ω. A good agreement is obtained between the measured values and the calculation. The maximum power point is calculated at a resistive load of 13.9 MΩ. It occurs when the value of the resistive load, $R_{load\ optimal}$, is equal to the impedance of the piezoelectric capacitor, at $R_{load\ optimal} = 1\ /\ \omega C_{piezo}$. This is confirmed by calculating the relative power as a function of the ratio between the resistive load and the impedance of the internal capacitance, presented in Fig. S6b.
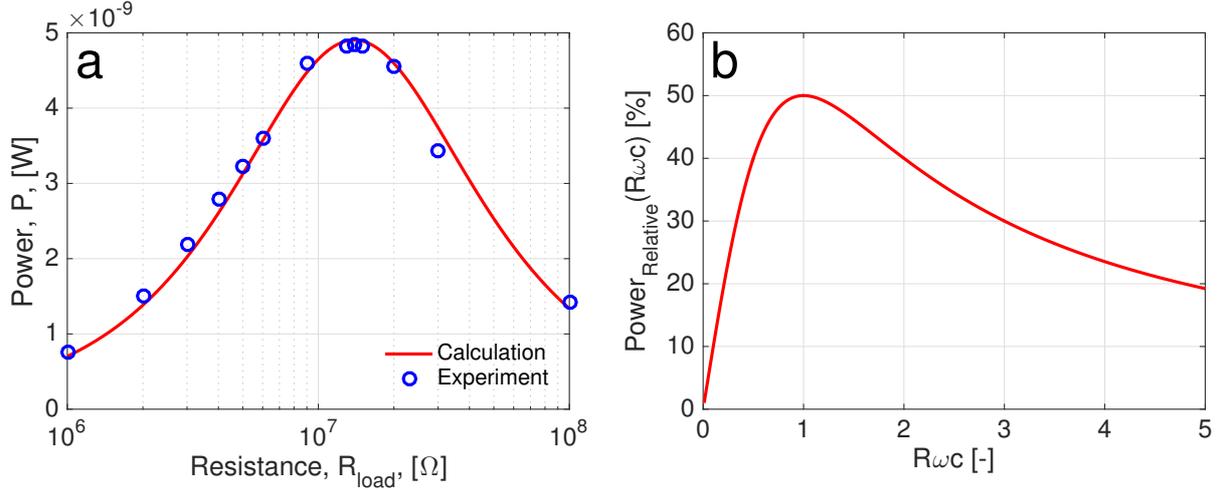
Figure S6. *Energy harvesting output of a piezoelectric capacitor. (a) The power output of a PZ27 ceramic as a function of the resistive load, actuated with a sinusoidal excitation at 10 Hz, and 3 N peak to peak. The red line is calculated with eqn. (S27). The open circles represent measurements of a PZ27 ceramic disk. (b) The dependence of the relative power output on the ratio between the applied resistive load, R, and the impedance of the internal capacitance, Z =1 / jωC, calculated with eqn. (S26), with normalized x-axes to $R_{load}ωC$.*

To identify the electrical-electrical conversion efficiency, the power obtained with the resistive load can be compared to the internal power in open circuit, P_{open}, where $V_{open}(\omega t)$ is the voltage in open circuit $V_{open}(\omega t) = V_{max} f(\omega t)$.

$$P_{open} = \frac{\left(\frac{V_{open}}{\sqrt{2}}\right)^2}{\omega C_{piezo}} \tag{S28}$$

The term 'open circuit power' is thermodynamically not defined. However, here we used this artificial term to clearly distinguish between the internal energy stored in the piezoelectric transducer, P_{open}, and the energy that can be externally dissipated in the load, $P_{harvested}$.

The maximum power is obtained when $R\omega C_{piezo}$ is 1, or the value of the resistive load is equal to $1 / \omega C_{piezo}$ (Fig. S6), and is equal to 50% P_{open}. In summary, at $R_{load} = 1 / \omega C_{piezo}$ the relationship between the open circuit voltage (taken from eqn. (S28)) and the harvested voltage (taken from eqn. (S27)) reduces to:

$$V_{harvested} = \frac{1}{\sqrt{2}} V_{open} \tag{S29}$$

The powers scale with the square of the voltage, meaning that:

$$P_{harvested} = \left(\frac{1}{\sqrt{2}}\right)^2 P_{open} = \frac{1}{2} P_{open} \tag{S30}$$

or, half of the internal open circuit power is transferred to harvested power when using a resistive load.

References

1. S. Roundy, *Journal of Intelligent Material Systems and Structures*, 2005, **16**, 809-823.

2. K. Uchino, *Ferroelectric devices & Piezoelectric actuators*, DEStech Publications Inc. , Lancaster, PA, USA, 10 edn., 2017.

3. Q. M. Wang, X. H. Du, B. Xu and L. E. Cross, *IEEE Transactions on Ultrasonics, Ferroelectrics and Frequency Control*, 1999, **46**, 638-646.

4. O. Guillon, F. Thiebaud and D. Perreux, *International Journal of Fracture*, 2002, **117**, 235-246.

5. E. Lefeuvre, A. Badel, A. Benayad, L. Lebrun, C. Richard and D. Guyomar, *Journal de Physique IV (Proceedings)*, 2005, **128**, 177-186.

6. S. Roundy, P. K. Wright and R. J., *Compute Communications*, 2003, **26**, 1131-1144.

7. W. C. Young and R. G. Budynas, *Roark's formulas for stress and strain*, McGraw-Hill, New York, USA, 7th edn., 2002.

8. R. C. Hibbeler, *Mechanics of materials*, Prentice Hall, Singapore, SI Second Edition edn., 2005.

9. D. Damjanovic, *Journal of Applied Physics*, 1997, **82**, 1788-1797.

10. M. E. Lines and A. M. Glass, *Principles and applications of ferroelectrics and related materials*, Oxford university press, 1977.

11. M. Stengel, N. A. Spaldin and D. Vanderbilt, *Nature Physics*, 2009, **5**, 304-308.

12. A. F. Devonshire, *The London, Edinburgh, and Dublin Philosophical Magazine and Journal of Science*, 1951, **42**, 1065-1079.

13. I. Katsouras, K. Asadi, M. Li, T. B. Van Driel, K. S. Kjær, D. Zhao, T. Lenz, Y. Gu, P. W. M. Blom, D. Damjanovic, M. M. Nielsen and D. M. de Leeuw, *Nature materials*, 2016, **15**, 78-84.

14. R. E. Newnham, V. Sundar, R. Yimnirun, J. Su and Q. M. Zhang, *Journal of Phyiscal Chemistry B*, 1997, **101**, 10141-10150.

15. F. Li, L. Jin, Z. Xu and S. Zhang, *Applied Physics Reviews*, 2014, **1**, 011103.

16. F. Li, L. Jin and R. Guo, *Applied Physics Letters*, 2014, **105**, 232903.

17. M. Jambunathan, R. Elfrink, R. Vullers, R. van Schaijk, M. Dekkers and J. Broekmaat, 2012.

18. M. W. Shafer and E. Garcia, *Journal of Vibration and Acoustics*, 2013, **136**, 021007.

19. E. E. Aktakka, H. Kim and K. Najafi, *Journal of Micromechanics and Microengineering*, 2011, **21**, 095016.

20. M. Renaud, R. Elfrink, M. Jambunathan, C. de Nooijer, Z. Wang, M. Rovers, R. Vullers and R. van Schaijk, *Journal of Micromechanics and Microengineering*, 2012, **22**, 105030.

21. J. M. Renno, M. F. Daqaq and D. J. Inman, *Journal of Sound and Vibration*, 2009, **320**, 386-405.

22. E. Halvorsen, *Journal of Microelectromechanical Systems*, 2008, **17**, 1061-1071.